

Title	Observation of new neutron-deficient isotopes with $Z \geq 92$ in multinucleon transfer reactions
Author(s)	Devaraja H. M., Heinz S., Beliuskina O., Comas V. F., Hofmann S., Hornung C., Münzenberg G., Nishio Katsuhisa, Ackermann D., Gambhir Y. K., Gupta M., Henderson R. A., Heßberger F. P., Khuyagbaatar J., Kindler B., Lommel B., Moody K. J., Maurer J., Mann R., Popeko A. G., Shaughnessy D. A., Stoyer M. A., Yeremin A. V.
Citation	Physics Letters B, 748, p.199-203
Text Version	Publisher's Version
URL	<a href="https://jopss.jaea.go.jp/search/servlet/search?5052590">https://jopss.jaea.go.jp/search/servlet/search?5052590</a>
DOI	<a href="https://doi.org/10.1016/j.physletb.2015.07.006">https://doi.org/10.1016/j.physletb.2015.07.006</a>
Right	©2015 Published by Elsevier B.V. This is an open access article under the CC BY license ( <a href="http://creativecommons.org/licenses/by/4.0/">http://creativecommons.org/licenses/by/4.0/</a> ). Funded by SCOAP3.



## Observation of new neutron-deficient isotopes with $Z \geq 92$ in multinucleon transfer reactions



H.M. Devaraja<sup>a,b</sup>, S. Heinz<sup>a,c,\*</sup>, O. Beliuskina<sup>a,c</sup>, V. Comas<sup>a</sup>, S. Hofmann<sup>a</sup>, C. Hornung<sup>c</sup>, G. Münzenberg<sup>a,b</sup>, K. Nishio<sup>d</sup>, D. Ackermann<sup>a</sup>, Y.K. Gambhir<sup>b</sup>, M. Gupta<sup>b</sup>, R.A. Henderson<sup>e</sup>, F.P. Heßberger<sup>a</sup>, J. Khuyagbaatar<sup>a</sup>, B. Kindler<sup>a</sup>, B. Lommel<sup>a</sup>, K.J. Moody<sup>e</sup>, J. Maurer<sup>a</sup>, R. Mann<sup>a</sup>, A.G. Popeko<sup>f</sup>, D.A. Shaughnessy<sup>e</sup>, M.A. Stoyer<sup>e</sup>, A.V. Yeremin<sup>f</sup>

<sup>a</sup> GSI Helmholtzzentrum für Schwerionenforschung GmbH, 64291 Darmstadt, Germany

<sup>b</sup> Manipal Centre for Natural Sciences, Manipal University, Manipal 576014, Karnataka, India

<sup>c</sup> Justus-Liebig-Universität Giessen, II. Physikalisches Institut, 35392 Giessen, Germany

<sup>d</sup> Japan Atomic Energy Agency, Tokai, Ibaraki, 319-1195, Japan

<sup>e</sup> Lawrence Livermore National Laboratory, Livermore, CA 94551, USA

<sup>f</sup> Joint Institute for Nuclear Research, 141980 Dubna, Russia

### ARTICLE INFO

#### Article history:

Received 5 May 2015

Received in revised form 14 June 2015

Accepted 3 July 2015

Available online 8 July 2015

Editor: V. Metag

#### Keywords:

New isotopes

Heavy ion collisions

Deep inelastic transfer reactions

Alpha decay

### ABSTRACT

In deep inelastic multinucleon transfer reactions of  $^{48}\text{Ca} + ^{248}\text{Cm}$  we observed about 100 residual nuclei with proton numbers between  $Z = 82$  and  $Z = 100$ . Among them, there are five new neutron-deficient isotopes:  $^{216}\text{U}$ ,  $^{219}\text{Np}$ ,  $^{223}\text{Am}$ ,  $^{229}\text{Am}$  and  $^{233}\text{Bk}$ . As separator for the transfer products we used the velocity filter SHIP of GSI while the isotope identification was performed via the  $\alpha$  decay chains of the nuclei. These first results reveal that multinucleon transfer reactions together with here applied fast and sensitive separation and detection techniques are promising for the synthesis of new isotopes in the region of heaviest nuclei.

© 2015 Published by Elsevier B.V. This is an open access article under the CC BY license (<http://creativecommons.org/licenses/by/4.0/>). Funded by SCOAP<sup>3</sup>.

### 1. Introduction

In the last decade intense discussions arose on the possibility to apply Deep Inelastic Transfer (DIT) reactions for the synthesis of new exotic heavy and superheavy isotopes. One region of interest is neutron-rich transactinide and superheavy nuclei which cannot be produced in complete fusion reactions due to the lack of sufficiently neutron-rich projectile-target combinations. The other goal is to produce new isotopes and study their decay properties in the region of astrophysical interest along the closed  $N = 126$  neutron shell [1,2]. These nuclei are presently produced in fragmentation reactions at relativistic energies, however, fragmentation does not allow to reach nuclei above  $Z = 92$  because the available beams in present facilities are limited to uranium. Multinucleon transfer reactions might be an appropriate solution. They allow, in principle, to produce neutron-rich as well as neutron-deficient isotopes with

proton numbers reaching far beyond uranium. The topic itself is not new. Experimental and theoretical studies of DIT reactions in heavy systems at Coulomb barrier energies with the goal to produce heavy nuclei were already performed in the 1970s up to the 1990s [3–6]. The lowest cross-sections reached in some of those experiments were 20 nb. No new isotopes were observed. A revival of the topic was initiated about 10 years ago by new calculations (e.g. [7,8]) and measurements (e.g. [9]) of reaction cross-sections and also by the necessity to find methods different from the established fusion and fragmentation reactions which are exploited in the region of transuranium and superheavy nuclei. Meanwhile, the possible application of DIT for synthesis of new heavy nuclei has become a topical subject in various laboratories and appropriate separation and detection techniques are being developed. However, one has to keep in mind that the expected production cross-sections for new heavy and superheavy isotopes reach far below the microbarn range. As a consequence, similarly efficient separation and detection techniques have to be applied as used for the identification of single atoms from fusion-evaporation reactions in superheavy element experiments. The techniques have also

\* Corresponding author at: GSI Helmholtzzentrum für Schwerionenforschung GmbH, 64291 Darmstadt, Germany.

E-mail address: [s.heinz@gsi.de](mailto:s.heinz@gsi.de) (S. Heinz).

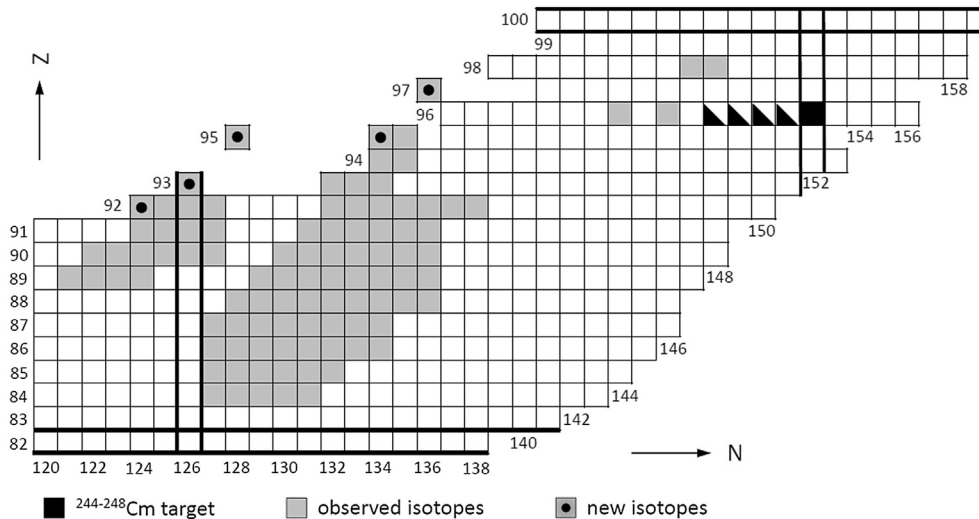


**Fig. 1.** Survey of all multinucleon transfer products (grey squares) which we identified in reactions of  $^{48}\text{Ca} + ^{248}\text{Cm}$ . Beside  $^{248}\text{Cm}$  with a contribution of 96.85% (black square), the target contained also the isotopes  $^{244-247}\text{Cm}$  with contributions of 0.0007%, 0.031%, 3.10% and 0.015% (black triangles). The new isotopes are marked by dots. The isotopes close to the valley of beta stability were observed with the largest yields of up to few hundred events in about 5 h of irradiation while for the new isotopes we observed one decay chain in each case.

to be fast due to the short half-lives of exotic nuclei. Up to now no dedicated in-flight separators exist for heavy DIT products. In this letter we report the successful application of a velocity filter, which is usually used to separate heavy fusion-evaporation residues, for separation of heavy DIT products from the primary beam. The isotope identification was performed via  $\alpha$  decay tagging. The sensitivity of this method allowed us to detect DIT products with cross-sections on the sub-nanobarn scale and with half-lives down to 2  $\mu\text{s}$ , which enabled the observation of several new neutron-deficient isotopes in the region  $Z \geq 92$ .

## 2. Experimental setup and method

The  $^{48}\text{Ca}$  beam was delivered by the UNILAC accelerator of GSI with an average intensity of  $2.0 \cdot 10^{12}$  projectiles/s and an energy of 270 MeV for reactions in the middle of the target. The structure of the UNILAC beam consisted of 5 ms long pulses followed by 15 ms long beam-off periods. The targets consisted of  $460 \mu\text{g}/\text{cm}^2$  thick layers of  $^{248}\text{Cm}$  oxide which were deposited on titanium backing foils with a thickness of (2.2–2.4)  $\mu\text{m}$ . We used the velocity filter SHIP [10] to separate the target-like DIT products of interest from the primary beam and other reaction products. SHIP accepts nuclei which are emitted in forward angles of  $(0 \pm 2)$  degree. Nuclei which pass SHIP are implanted in a position sensitive silicon strip detector (stop detector) to measure the energy, position and time of implantation of the nuclei and their decay products [11]. Particularly in this experiment, the  $\alpha$  decay chains were reconstructed to allow an unambiguous assignment of the produced nuclei. Six further silicon detectors are installed in a box-like arrangement in front of the stop detector (box detector) and cover 85% of the backward hemisphere in order to register  $\alpha$  particles and spontaneous fission fragments escaping from the stop detector. Two time-of-flight detectors were mounted upstream of the box detector. They are used to distinguish residual nuclei produced in the reaction from  $\alpha$  particles and fission fragments emitted from implanted nuclei in the stop detector.

The target-like DIT products which are emitted in forward direction have velocities close to two times the compound nucleus velocity (i.e. centre-of-mass velocity)  $v_{\text{CN}}$ . The velocity depends on A, Z and the energy dissipation during the reaction. We applied five different field settings of SHIP to transmit reaction products

with velocities  $1.70 v_{\text{CN}}$ ,  $1.80 v_{\text{CN}}$ ,  $1.85 v_{\text{CN}}$ ,  $1.90 v_{\text{CN}}$  and  $1.95 v_{\text{CN}}$ . At each setting we measured the  $\alpha$  spectra and spontaneous fission decays of the nuclei which were implanted in the stop detector. The lowest background is achieved during beam-off periods. The experiment was very sensitive and allowed to reach lower limit cross-sections of  $\sim 50$  pb for the detection of one event in five hours of irradiation, at the above given beam current and target thickness. The lowest accessible half-lives of 20  $\mu\text{s}$  were given by the conversion time plus dead time of the data acquisition system.

## 3. Experimental results

The grey squares in Fig. 1 represent all target-like reaction products which we identified in our experiment. Usually, a contiguous region of isotopes around the target and projectile nucleus is populated in DIT reactions. The nuclei which are represented by the blank squares in Fig. 1 cannot be detected in our experiment due to too short or long half-lives and/or unfavourable decay channels like fission or beta decay. Apart from a large number of already known nuclei our data revealed several new isotopes which are located in the region  $Z \geq 92$  on the neutron-deficient side of the nuclear chart. All of them lead to decay chains of already known nuclei which enabled their assignment. Five new isotopes which we identified are marked by dots in Fig. 1. The respective decay chains are shown in Fig. 2 while the  $\alpha$  decay energies and half-lives of the new isotopes are listed in Table 1.

### 3.1. The new isotope $^{216}\text{U}$

The most neutron-deficient so far known isotope of uranium is  $^{217}\text{U}$ . In our experiment we identified three decay chains of this isotope produced in DIT reactions. Further, we observed one sequence of three  $\alpha$  decays which we assigned to the decay chain of the new isotope  $^{216}\text{U}$  (chain (a) in Fig. 2). The  $\alpha$  energies and half-lives of  $\alpha_2$  and  $\alpha_3$  are, within statistical error bars, in agreement with the ones of the known decay products  $^{212}\text{Th}$  and  $^{208}\text{Fr}$ . Preceding  $^{212}\text{Th}$ , we observed an  $\alpha$  decay with an energy of 8335 keV following an implanted recoil nucleus after 5.5 ms. It is noteworthy that after  $^{212}\text{Th}$  we do not observe the  $\alpha$  decay of  $^{208}\text{Ra}$  but one which is very well in agreement with  $^{208}\text{Fr}$ . This can be explained with the electron capture (EC) branch (5%) of  $^{208}\text{Ra}$  which

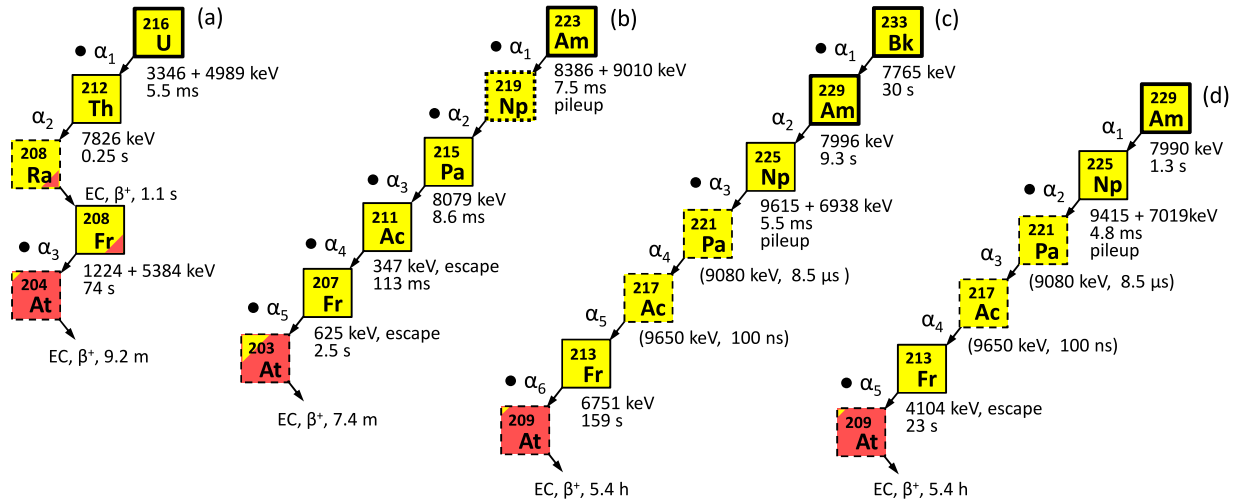


**Fig. 2.** Decay chains of the new isotopes which we observed in multinucleon transfer reactions of  $^{48}\text{Ca} + ^{248}\text{Cm}$ . The squares framed with full lines mark isotopes which were observed in the experiment while dashed frames indicate isotopes which are expected members of the respective decay chain but were not observed. The new isotopes are marked by squares with bold frames. Bullets indicate  $\alpha$  decays which occurred during beam-off periods. All observed events within a chain were correlated in position within less than  $\pm 0.5$  mm. The measured  $\alpha$  decay energies and lifetimes  $\tau$  are given for each observed nucleus. In the case of coincident energy signals from stop and box detector we show both contributions. Energies and half-lives in brackets represent literature values. Each chain was preceded by a recoil nucleus in the time denoted at  $\alpha_1$  and terminated with an EC or  $\beta^+$  decay, respectively, which is not observable with our method.

leads to  $^{208}\text{Fr}$ . Despite the relatively long correlation time of 51 s, a random correlation is unlikely since the random coincidence rate is estimated to be one event in 30 min in the energy window  $(6636 \pm 50)$  keV with constraints on the position of  $\pm 0.25$  mm with respect to the position of the observed  $\alpha_3$ .

### 3.2. The new isotopes $^{223}\text{Am}$ and $^{219}\text{Np}$

Decay chain (b) can be attributed to the new isotope  $^{223}\text{Am}$ . The decay sequence consists of an implanted recoil nucleus followed by a pileup  $\alpha$  event with 17.4 MeV and three further  $\alpha$  decays. The pileup of  $\alpha_1$  and  $\alpha_2$  is due to the expected short half-life of the daughter nucleus  $^{219}\text{Np}$  which is also a new isotope. The decay must have been occurred within a time smaller than the coincidence time of our readout system which is 5  $\mu\text{s}$ . A fraction of 8386 keV of the total pileup energy was deposited in the stop detector while the remaining 9010 keV were deposited in the box detector. From this we can estimate a lower limit for the  $\alpha$  energy of  $^{219}\text{Np}$  of 9000 keV which is given by the scenario where the full energy of the  $^{223}\text{Am}$   $\alpha$  is deposited in the stop detector and only the Np  $\alpha$  escapes to the box detector. All other possible scenarios lead to  $\alpha$  energies smaller than 9000 keV. The last two decays in the sequence,  $\alpha_4$  and  $\alpha_5$ , were registered with energies 347 keV and 625 keV. They can most likely be attributed to escape  $\alpha$ 's from the decays of  $^{211}\text{Ac}$  and  $^{207}\text{Fr}$ . This is supported by the respective correlation times which are in accordance with the half-lives of  $^{211}\text{Ac}$  and  $^{207}\text{Fr}$ .

### 3.3. The new isotopes $^{233}\text{Bk}$ and $^{229}\text{Am}$

We attributed decay chain (c) to the new isotope  $^{233}\text{Bk}$ . The observed half-lives of  $^{233}\text{Bk}$  and its daughter nucleus  $^{229}\text{Am}$ , which is also a new isotope, are well in agreement with WKB calculations using the measured  $\alpha$  energies. This attribution is supported by the last decay in chain (c) which is well in agreement with  $^{213}\text{Fr}$ . A random correlation with  $^{213}\text{Fr}$  is unlikely. The random coincidence rate was one event in  $\sim 20$  min for the relatively broad energy window of  $(6775 \pm 50)$  keV and constraints on the position of  $\pm 0.5$  mm with respect to the position where the decay  $\alpha_6$  occurred. This is 8 times longer than the measured correlation time

of 159 s. The third event in the chain is a pileup event with energy 16.6 MeV. Actually, we would expect a pileup energy of  $\sim 27$  MeV because  $^{225}\text{Np}$  is followed by two very short-living nuclei,  $^{221}\text{Pa}$  ( $\tau = 8.5 \mu\text{s}$ ) and  $^{217}\text{Ac}$  ( $\tau = 100$  ns). Their decay energies add up with the  $\alpha$  energy of  $^{225}\text{Np}$ . The apparently too low pileup energy which we measure can be explained if we assume that the decay of  $^{221}\text{Pa}$  occurs shortly before the end of the coincidence time of our data acquisition system and therefore not the full pileup energy of  $^{221}\text{Pa}$  and  $^{217}\text{Ac}$  is registered.

The two  $\alpha$  decays  $\alpha_1$  and  $\alpha_2$  in chain (d) are very well in agreement with the decays of  $^{229}\text{Am}$  and  $^{225}\text{Np}$  in chain (c). The half-life of the escape event  $\alpha_5$  is well in agreement with the one of  $^{213}\text{Fr}$ . Therefore we assigned the chain to the decay of  $^{229}\text{Am}$  which is in this case directly produced in the DIT reaction.

### 3.4. Cross-sections of the new isotopes

To obtain total production cross-sections for the new isotopes produced in DIT reactions, one has to take into account their angular and energy distributions which determine the fraction of nuclei which is accepted by SHIP. Experimental data for the efficiency of those products which reach the focal plane of SHIP are not available. Therefore, we rely on the efficiencies obtained from calculations in the dinuclear system model [16] for our collision system and beam energy. For the simulation it was assumed that the target-like DIT products are emitted isotropically in the centre-of-mass system. In the laboratory system they are emitted in an opening angle of about  $\pm 60$  degree. The total efficiency which takes also into account an assumption on the charge distribution is  $\sim 0.5\%$ . With this we obtain total cross-sections of  $\sim 5$  nb for the observed isotopes. Only a rough estimate of the error bars is possible. It is dominated by the uncertainty in the angular efficiency of SHIP for DIT products which is based on model dependent theoretical calculations. Therefore, fluctuations of a factor 5 to 10 might be possible.

Cross-sections on the nanobarn scale are also obtained in fusion-evaporation reactions for isotopes in this region. For example,  $^{217}\text{U}$  was produced in fusion-evaporation reactions of  $^{40}\text{Ar} + ^{182}\text{W}$  with a cross-section of 1 nb [17] and for  $^{228}\text{Pu}$  fusion-

**Table 1**

Alpha-decay energies and half-lives of the new isotopes produced in multinucleon transfer reactions of  $^{48}\text{Ca} + ^{248}\text{Cm}$  (columns 3 and 5). The measured  $\alpha$  energies and half-lives of the observed daughter nuclei are also shown. The half-lives were calculated from the measured correlation times (i.e. lifetimes  $\tau$ ) given in Fig. 2 according to  $T_{1/2} = \tau \ln(2)$ . Literature values are given in columns 4 and 6. References for the literature values are in column 8. The error bars for the measured  $\alpha$  energies, including systematic errors, are  $\pm 0.02$  MeV if the event occurred only in the stop detector and  $\pm 0.05$  MeV for coincident energy signals in the stop and box detector. The given statistical errors for the half-lives, which were calculated according to method [12], correspond to one standard deviation. WKB calculations of half-lives (for  $\Delta\ell = 0$ ) using the measured  $\alpha$  energies are shown in column 7. In case of escape or pileup events the literature values were used for the calculation. The velocity settings of SHIP at which the new isotopes were observed are given in column 2.

Isotope	SHIP setting	$E_{\alpha}$ /MeV	$E_{\alpha, lit}$ /MeV	$T_{1/2}$	$T_{1/2, lit}$	$T_{1/2, WKB}$	Reference
$^{216}_{92}\text{U}$	1.95 $v_{CN}$	$8.34 \pm 0.05$		$3.8^{+8.8}_{-3.2}$ ms		3.1 ms	this work
$^{212}_{90}\text{Th}$		$7.83 \pm 0.02$	7.809	$173^{+398}_{-143}$ ms	31.7 ms	22 ms	[13]
$^{208}_{87}\text{Fr}$		$6.61 \pm 0.05$	6.636	$51^{+117}_{-42}$ s	58.6 s	30 s	[14]
$^{223}_{95}\text{Am}$	1.80 $v_{CN}$	17.4, pileup		$5.2^{+12.0}_{-4.4}$ ms			this work
$^{219}_{93}\text{Np}$		> 9				< 98 $\mu\text{s}$	this work
$^{215}_{91}\text{Pa}$		$8.08 \pm 0.02$	8.085	$6.0^{+13.8}_{-5.0}$ ms	14 ms	8.1 ms	[15]
$^{211}_{89}\text{Ac}$		0.347, escape	7.481	$78^{+179}_{-64}$ ms	250 ms	125 ms	[14]
$^{207}_{87}\text{Fr}$		0.625, escape	6.767	$1.7^{+3.9}_{-1.4}$ s	14.8 s	7.6 s	[14]
$^{229}_{95}\text{Am}$	1.95 $v_{CN}$	$7.99 \pm 0.02$		$0.9^{+2.1}_{-0.7}$ s		0.3 s	this work
$^{225}_{93}\text{Np}$		16.4, pileup	8.63	$3.3^{+7.6}_{-2.7}$ ms		0.78 ms	[14]
$^{213}_{87}\text{Fr}$		4.10, escape	6.775	$16^{+37}_{-13}$ s	34.6 s	5.6 s	[14]
$^{233}_{97}\text{Bk}$	1.95 $v_{CN}$	$7.77 \pm 0.02$		$21^{+48}_{-17}$ s		9.5 s	this work
$^{229}_{95}\text{Am}$		$8.00 \pm 0.02$		$6.4^{+14.9}_{-5.4}$ s		0.3 s	this work
$^{225}_{93}\text{Np}$		16.6, pileup	8.63	$3.8^{+7.6}_{-2.7}$ ms		0.78 ms	[14]
$^{213}_{87}\text{Fr}$		$6.75 \pm 0.02$	6.775	$110^{+250}_{-90}$ s	34.6 s	7.0 s	[14]

evaporation cross-sections of 2 nb were measured in reactions of  $^{34}\text{S} + ^{198}\text{Pt}$  [18].

#### 4. Conclusions and outlook

Our results revealed that the application of deep inelastic transfer reactions is promising for the production of new heavy isotopes. In DIT reactions of  $^{48}\text{Ca} + ^{248}\text{Cm}$  we identified nuclei which reach out to the limits of the present chart of nuclides on the neutron-deficient side. It is remarkable that the isotopic distributions, which we so far deduced from our data, do not show the steep drops observed in Fig. 1 of Ref. [5] if one moves away from the maximum, but reveal broad tails towards the neutron-deficient side. A likely reason for this is the narrow acceptance angle of SHIP in forward direction which leads to the selection of reaction products from central collisions with very small angular momenta. Under these conditions, projectile and target nucleus have relatively large nuclear overlap and long interaction times which enables the exchange of a large number of nucleons leading to isotopes far from the target. On the other hand, SHIP suppresses events from more grazing collisions and with this, reaction products which are located closer to the target nucleus.

For the four new decay chains which we observed, we made the best possible assignment on basis of the decay properties of already known nuclei and on WKB calculations of the half-lives. Assignments different from the ones in Fig. 2 lead to inconsistencies. With one exception, the nuclei were observed at 1.95  $v_{CN}$ , the largest velocity setting in this experiment. This is consistent with expectations for DIT products well below the target, while heavier nuclei close to and above the target have lower velocities around 1.70  $v_{CN}$ . A detailed discussion of the new decay chains, measured isotopic distributions, systematics of decay properties and comparison with previous experiments will be presented in a forthcoming paper. In a follow-up experiment we will use fast digital electronics which was not available in the present experiment. This will allow to access correlation times down to 100 ns and with this to

resolve the events which appeared as pileups in the present experiment.

The cross-sections of neutron-deficient isotopes from DIT are comparable to those measured in fusion-evaporation reactions. An advantage of DIT reactions is that the excitation functions of DIT products are relatively broad and a vast region of isotopes can be populated at a given beam energy while fusion-evaporation reactions are selective only on few isotopes at a given experimental setting. On the other side, DIT products have broad angular distributions which result in relatively small angular efficiencies on the level of few percent or less for existing in-flight separators while the angular efficiencies for fusion-evaporation residues are typically more than 10 times larger.

Our results further show that existing velocity filters for heavy fusion-evaporation residues can also be used in the search for new exotic DIT products. The accessibility of new isotopes is in fact limited by their decay properties. In particular, nuclei which undergo beta decay or fission as well as very long-living nuclei cannot be identified with the available detection techniques. Therefore, in future experimental setups for heavy and superheavy DIT products special emphasis must be put on the development of detection techniques which allow the identification of the nuclei independent of their decay properties. A possibility might be precision mass measurements with Penning traps or multiple reflection time-of-flight spectrometers where a resolving power of ( $10^5$ – $10^6$ ) is already sufficient for an isobaric separation of most of the isotopes.

#### Acknowledgements

We would like to thank the crew of the UNILAC accelerator for the excellent technical support throughout the experiment. Further, we thank our colleagues from theory G. Adamian, N. Antonenko, W. Greiner, J. Maruhn, and V. Zagrebaev for providing us with model calculations and for fruitful discussions. In particular, we dedicate this work to Prof. Valery Ivanovich Zagrebaev who passed away so unexpected and much too early in January 2015.

He encouraged and motivated us strongly to perform these experiments and accompanied us continuously with theoretical calculations.

This work was performed in the frame of our collaboration between GSI, Manipal University and Justus-Liebig-University Giessen. One of us, H.M. Devaraja, was supported by HIC for FAIR.

## References

- [1] J. Benlliure, H. Alvarez-Pol, T. Kurtukian-Nieto, A.I. Morales, L. Audouin, F. Becker, B. Blank, I. Borzov, E. Casarejos, D. Cortina-Gil, et al., *J. Phys. Conf. Ser.* 337 (2012) 012070.
- [2] J. Kurcewicz, F. Farinon, H. Geissel, S. Pietri, C. Nociforo, A. Prochazka, H. Weick, J.S. Winfield, A. Estrade, P.R.P. Allegro, et al., *Phys. Lett. B* 717 (2012) 371.
- [3] H. Freiesleben, K.D. Hildenbrand, F. Pühlhofer, W.F.W. Schneider, R. Bock, *Z. Phys. A* 292 (1979) 171.
- [4] M. Schädel, W. Brühle, H. Gäggeler, J.V. Kratz, K. Sümmerer, G. Wirth, G. Herrmann, R. Stakemann, G. Tittel, N. Trautmann, et al., *Phys. Rev. Lett.* 48 (1982) 852.
- [5] H. Gäggeler, W. Brühle, M. Brügger, M. Schädel, K. Sümmerer, G. Wirth, J.V. Kratz, M. Lerch, T. Blaich, G. Herrmann, et al., *Phys. Rev. C* 33 (1986) 1983.
- [6] A. Türler, H.R. von Gunten, J.D. Leyba, D.C. Hoffman, D.M. Lee, K.E. Gregorich, D.A. Bennett, R.M. Chasteler, C.M. Gannett, H.L. Hall, et al., *Phys. Rev. C* 46 (1992) 1364.
- [7] G.G. Adamian, N.V. Antonenko, A.S. Zubov, *Phys. Rev. C* 71 (2005) 034603.
- [8] Valery Zagrebaev, Walter Greiner, *J. Phys. G* 35 (2008) 125103.
- [9] L. Corradi, A.M. Vinodkumar, A.M. Stefanini, E. Fioretto, G. Prete, S. Beghini, G. Montagnoli, F. Scarlassara, G. Pollarolo, F. Cerutti, A. Winther, *Phys. Rev. C* 66 (2002) 024606.
- [10] G. Münzenberg, W. Faust, S. Hofmann, P. Armbruster, K. Güttner, H. Ewald, *Nucl. Instrum. Methods* 161 (1979) 65.
- [11] S. Hofmann, G. Münzenberg, *Rev. Mod. Phys.* 72 (2000) 733.
- [12] K.-H. Schmidt, C.C. Sahn, K. Pielenz, H.G. Clerc, *Z. Phys. A* 316 (1984) 19.
- [13] J.A. Heredia, A.N. Andreyev, S. Antalic, S. Hofmann, D. Ackermann, V.F. Comas, S. Heinz, F.P. Heßberger, B. Kindler, J. Khuyagbaatar, et al., *Eur. Phys. J. A* 46 (2010) 337.
- [14] J. Magill, G. Pfennig, R. Dreher, Z. Soti, *Chart of the Nuclides*, 8th edition, 2012.
- [15] K.-H. Schmidt, W. Faust, G. Münzenberg, H.-G. Clerc, W. Lang, K. Pielenz, D. Vermeulen, H. Wohlfahrt, H. Ewald, K. Güttner, *Nucl. Phys. A* 318 (1979) 253.
- [16] G.G. Adamian, N.V. Antonenko, *private communication*.
- [17] O.N. Malyshev, A.V. Belozerov, M.L. Chelnokov, V.I. Chepigin, V.A. Gorshkov, A.P. Kabachenko, A.G. Popeko, J. Rohach, R.N. Sagaidak, A.V. Yeremin, et al., *Eur. Phys. J. A* 8 (2000) 295.
- [18] K. Nishio, H. Ikezoe, S. Mitsuoka, K. Satou, C.J. Lin, *Phys. Rev. C* 68 (2003) 064305.